

Oriented Reconstitution of a Membrane Protein in a Giant Unilamellar Vesicle: Experimental Verification with the Potassium Channel KcsA

Miho Yanagisawa,^{*,†,||} Masayuki Iwamoto,[‡] Ayako Kato,^{†,§} Kenichi Yoshikawa,^{*,†} and Shigetoshi Oiki^{*,‡}

[†]Department of Physics, Graduate School of Science, Kyoto University, Kyoto 606-8501, Japan

[‡]Department of Molecular Physiology and Biophysics, Faculty of Medical Sciences, University of Fukui, Fukui 910-1193, Japan

[§]Graduate School of Pharmaceutical Sciences, Josai University, Saitama 350-0295, Japan

 Supporting Information

ABSTRACT: We report a method for the successful reconstitution of the KcsA potassium channel with either an outside-out or inside-out orientation in giant unilamellar vesicles, using the droplet-transfer technique. The procedure is rather simple. First, we prepared water-in-oil droplets lined with a lipid monolayer. When solubilized KcsA was encapsulated in the droplet, it accumulated at monolayers of phosphatidylglycerol (PG) and phosphoethanolamine (PE) but not at a monolayer of phosphatidylcholine (PC). The droplet was then transferred through an oil/water interface having a preformed monolayer. The interface monolayer covered the droplet so as to generate a bilayer vesicle. By creating chemically different lipid monolayers at the droplet and oil/water interface, we obtained vesicles with asymmetric lipid compositions in the outer and inner leaflets. KcsA was spontaneously inserted into vesicles from the inside or outside, and this was accelerated in vesicles that contained PE or PG. Integrated insertion into the vesicle membrane and the KcsA orientation were examined by functional assay, exploiting the pH sensitivity of the opening of the KcsA when the pH-sensitive cytoplasmic domain (CPD) faces toward acidic media. KcsA loaded from the inside of the PG-containing vesicles becomes permeable only when the intravesicular pH is acidic, and the KcsA loaded from the outside becomes permeable when the extravesicular pH is acidic. Therefore, the internal or external insertion of KcsA leads to an outside-out or inside-out configuration so as to retain its hydrophilic CPD in the added aqueous side. The CPD-truncated KcsA exhibited a random orientation, supporting the idea that the CPD determines the orientation. Further application of the droplet-transfer method is promising for the reconstitution of other types of membrane proteins with a desired orientation into cell-sized vesicles with a targeted lipid composition of the outer and inner leaflets.

INTRODUCTION

Experiments using the reconstituted membrane are indispensable for studying the mechanisms by which membrane proteins interact with lipids.¹ However, the available techniques for the reconstitution of membrane proteins into giant vesicles ($>5\ \mu\text{m}$) are limited, and their orientation cannot be adequately controlled with these methods.^{2,3} In some cases, the orientation of the integrated proteins is random,⁴ and in others, the orientation of all of the reconstituted proteins is either inside-out (the cytoplasmic side facing the outside of the vesicle) or outside-out,⁵ but an alternative orientation cannot be attained. This is a serious problem for studying membrane proteins, because certain membrane proteins are activated on only one side of the membrane, and transporter proteins transfer substances in one direction.

Here we present a novel method for incorporating membrane proteins into giant unilamellar vesicles (GUVs) in either orientation, as desired. To establish the method, we exploited the membrane protein KcsA as a model protein, because the functional features of KcsA are well-defined.^{6–12} KcsA is a K^+ channel protein from *Streptomyces lividans* which exhibits channel activity under the following conditions: (1) the cytoplasmic pH is acidic ($\text{pH} < 4$),⁷ and (2) the membrane contains anionic lipids, such as phosphatidylglycerol (PG).^{8,9} Interestingly, KcsA is incorporated almost exclusively into vesicles with an outside-out configuration,⁵ where

the pH-sensitive cytoplasmic domain (CPD) is located on the inside. This specific orientation has been attributed to the conical shape of the transmembrane domain,⁶ which matches the high curvature of small vesicles ($<500\ \text{nm}$) at the initial incorporation process,^{2,3} whereas such curvature dependence almost disappears in giant vesicles ($>10\ \mu\text{m}$) because the size of the protein is much smaller than the diameter of the giant vesicles. Because this orientation is retained as successive fusion proceeds, the reverse orientation, i.e., the inside-out configuration, cannot be achieved when this procedure is used. It is considered that gating would be readily controlled from outside the vesicles, if the inside-out orientation could be controlled.

In our method, incorporation of KcsA into GUVs in either orientation was realized using the droplet-transfer method.^{13–16} First, the localization of encapsulated KcsA within the droplets lined with a lipid monolayer is determined based on the lipid types and internal pH conditions (Figure 1A). Second, by transferring the droplets through the lipid monolayer, vesicles are prepared with an asymmetric lipid composition in their outer and inner leaflets.¹⁴ The lipid-dependence of KcsA insertion into bilayer vesicles and channel function are then examined

Received: May 14, 2011

Published: June 26, 2011

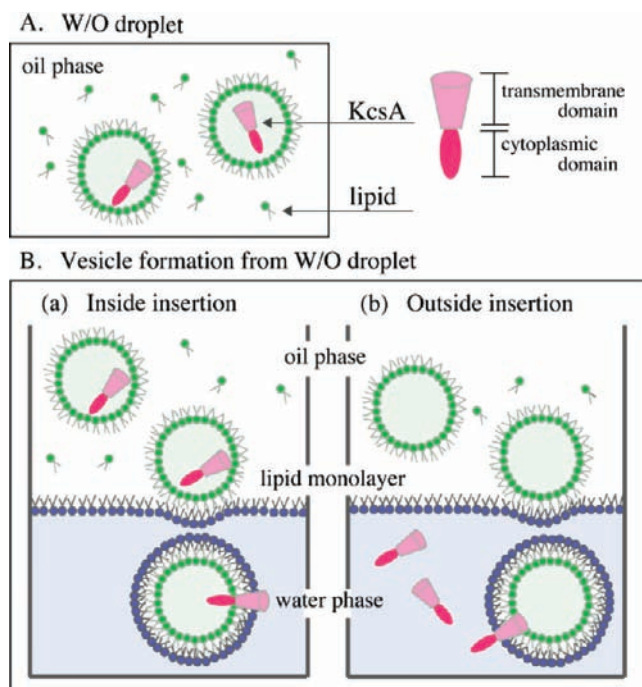


Figure 1. Schematic representation of the experimental procedure used to obtain vesicles containing KcsA in either orientation. (A) W/O (water-in-oil) droplets covered by a lipid monolayer (green) in the oil phase. (B) KcsA insertion into vesicles from (a) the inside and (b) outside, where the lipids of the outer leaflet (blue) are chemically different from those of the inner leaflet.

(Figure 1B). Finally, the incorporation of KcsA in either orientation is demonstrated to have successfully been achieved according to whether the insertion is internal or external. The novel method reported here may be applicable as a general methodology for reconstituting transmembrane proteins into cell-sized vesicles with a desired asymmetry of lipid compositions on the membrane leaflets and desired orientation of the proteins.

EXPERIMENTAL PROCEDURES

Purification and Fluorescence Labeling of KcsA. A mutant KcsA was generated by introducing a cysteine residue at the C-terminal end of the molecule (KcsA-161C), which has only a single cysteine residue throughout the entire molecule. KcsA-161C was expressed and purified as previously reported.¹¹ The cysteine residue of KcsA-161C was fluorescently labeled as follows. Purified KcsA-161C (20 μ M) which was dissolved in buffer (0.06% *n*-dodecyl- β -D-maltoside (DDM), 200 mM KCl, 10 mM HEPES, pH 7.5) was incubated with 200 μ M Alexa Fluor 532 C5-maleimide (Molecular Probes, Eugene, OR) at room temperature. After 2 h, 20 mM 2-mercaptoethanol was added to complete the reaction. Excess fluorescent dye was removed by passing the reaction mixture through a gel-filtration column (Bio-Spin 30 column, BioRad, Hercules, CA). The concentration of the fluorescent-labeled KcsA in the flow through (0.06% DDM, 200 mM KCl, 10 mM HEPES, pH 7.5) was 10 μ M, and this was used as the mother solution. From the absorption ratio of 532 nm/280 nm, one molecule of Alexa dye was expected to bind to one monomer of KcsA. The single-channel current of KcsA with or without the tag revealed that the fluorescent labeling did not alter the essential channel activity (Figure S1, Supporting Information).

Materials. Negatively charged lipid, 1,2-dioleoyl-*sn*-glycero-3-phosphatidylglycerol (DOPG) was obtained from Wako Pure Chemical Industries (Osaka, Japan). Egg yolk phosphatidylcholine (egg PC), 1,

2-dioleoyl-*sn*-glycero-3-phosphatidylcholine (DOPC), 1,2-dioleoyl-*sn*-glycero-3-phosphoethanolamine (DOPE), and 1,2-dihexanoyl-*sn*-glycero-3-phosphatidylethanolamine-*N*-(4-nitrobenzo-2-oxa-1,3-diazole) (NBD-PE) were purchased from Avanti Polar Lipids (Alabaster, AL). All lipids were used without further purification and stored in chloroform at -20 °C until use. Mineral oil and glucose/sucrose (Nacalai Tesque, Kyoto, Japan) were used to prepare water-in-oil (W/O) droplets and vesicles, respectively. Citric acid and disodium hydrogenorthophosphate (Nacalai Tesque) were used to control the pH, KCl, TINO₃, and KBr (Wako Pure Chemical Industries) were used as buffer solutions.

Preparation of W/O Droplets. The W/O droplet was prepared as described previously (Figure 1A).¹⁷ A dry film of lipids was made on the bottom of a glass tube. To visualize the distribution of the lipids, ~ 1 mol % of NBD-PE was added before preparing the lipid film. Mineral oil was added to the lipid film prior to sonication for ~ 90 min at 50 °C. The final lipid concentration in oil was 0.5–1 mM. This procedure resulted in dispersed lipids in oil. Next, to obtain W/O droplets, 5–10 vol % aqueous solution was added to the lipid/oil solution and emulsification was performed by pipetting. The diameter of the resulting W/O droplets ranged from 10 to 100 μ m. An aliquot of W/O droplets was placed on a silicone-coated coverslip for observation.

Preparation of Vesicles Transferred from the Droplets. We prepared giant unilamellar vesicles using the droplet-transfer method (Figure 1B).^{15,16} A thin layer in the water phase was introduced at the bottom of a cylindrical hole (ca. 4 mm in diameter) in a PDMS (polydimethylsiloxane) sheet (ca. 5 mm thick) and covered with a lipid/oil solution. After 1 h, a lipid monolayer was stably formed at the oil/water interface. Then, the oil phase of the W/O droplets was added just after emulsification above the lipid layer. To transfer the droplets, we added ~ 100 mM sucrose solution to the internal media and an equimolar glucose solution to the external media. The droplets in the oil phase then spontaneously crossed the lipid monolayer, driven by the difference in molar density, i.e., the gravity difference, between sucrose and glucose. During transfer, the droplets were converted to vesicles while maintaining asymmetry, where the monolayer that covers droplets becomes the inner leaflet of the vesicle, and the monolayer at the oil/water interface becomes the outer leaflet. The average diameter of the obtained vesicles was ~ 20 μ m.

Microscopic Observation. Bright-field and fluorescence microscopy images were obtained with a confocal laser scanning microscope (LSM510, Carl Zeiss, Jena, Germany). Alexa532-labeled KcsA was excited with an argon laser, and the images were obtained through a 505–530 nm band-pass filter. The pinhole size was fixed at ~ 3 μ m. All samples were observed within 1 h after the formation at room temperature (ca. 20 °C). All micrographs show cross-section images of the vesicles along their equators.

Crystallization. We developed a thallium (Tl) crystallization method to examine the channel activity of KcsA reconstituted in vesicles.¹⁸ A mixture of 10–20 mM TINO₃, 100 mM KCl, pH buffer, and 100 mM glucose was used as the outer media. A mixture of 10–20 mM KBr, 100 mM KCl, pH buffer, and 100 mM sucrose was used as the inner media. The osmolarity of the outer and inner media should be the same. If not, the W/O droplets will not be transferred to the vesicles but collapse at the bulk oil/water interface. The Tl⁺ is a permeable ion for most of the potassium channels, including KcsA.¹⁹ When the reconstituted KcsA opens the gate and permeates extraventricular Tl⁺ into the vesicles, Tl⁺ aggregates with intravesicular Br[−] and forms TlBr crystals. These crystals are observable using cross-polarized light. This crystallization experiment has been performed more than 20 times.

RESULTS AND DISCUSSION

Distribution of KcsA in the W/O Droplets. W/O droplets were obtained by mixing a lipid/oil solution and an aqueous

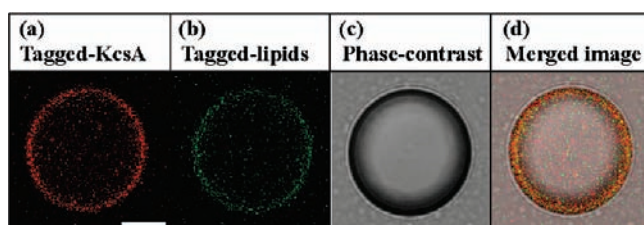


Figure 2. The distribution of KcsA channels within a W/O droplet lined by a DOPG monolayer. Confocal micrograms show (a) tagged-KcsA channels as a red-fluorescent image, (b) tagged-lipids as a green-fluorescent image, (c) the oil/water interface as a phase-contrast image, and (d) a merged image. Scale bar is 10 μm .

solution containing solubilized KcsA proteins and then emulsifying the mixed solution by pipetting. The water droplets lined with a lipid monolayer that range in size from 10 to 100 μm are seen in the oil phase. Figure 2 shows confocal images of a DOPG droplet containing KcsA (pH 7.0). In the fluorescent images (Figure 2a,b), the patterns of the tagged-KcsA and tagged-lipids are shown, respectively. The merged image (Figure 2d) demonstrates that the KcsA channels are localized near the lipid monolayer. This specific localization of tagged-KcsA or the tag Alexa at the interface was not observed on the droplets in the absence of lipids (Figure S5, Supporting Information). When the DDM concentration in the aqueous solution was increased from the 0.015% used in the above experimental results to 0.06%, KcsA was distributed homogeneously inside the droplet, which suggests that a DDM concentration below the critical micelle concentration facilitated the transfer of KcsA from the aqueous solution to the lipid monolayer.

To examine whether the distribution of KcsA depends on the type of lipid lining the droplet, four different kinds of W/O droplets coated with DOPG, DOPE, DOPC, or eggPC were obtained. In the confocal images, the profile of the fluorescence intensity along the equator of the droplet was examined (Figure 3A). In contrast to the sharp peak for the DOPG droplet, there are no peaks for the eggPC droplet. The distribution was ranked according to the following criteria. The normalized peak intensity I/I_0 , which is the ratio between the maximum peak and the background, was calculated for 30 droplets under each condition (Figure S6A, Supporting Information). From the histograms of the I/I_0 values (ranging from 0 to 15; $0 < I/I_0 < 15$), we obtained the average value I^* and categorized the distribution patterns into four types: $-$, $I^* \leq 1$; $+$, $1 < I^* \leq 5$; $++$, $5 < I^* \leq 10$; $+++$, $I^* > 10$.

Figure 3B (upper row) summarizes the results at neutral pH, where the channel structure is maintained in a closed conformation. While anionic DOPG and zwitterionic DOPE attracted KcsA, the other zwitterionic lipids, DOPC and eggPC, did not, at least within 2 h after the formation. The degree of accumulation at the interface was in the order $\text{PG} > \text{PE} \gg \text{PC}$. Although PE and PC are both zwitterionic lipids, it has been reported that the PE membrane has a net negative charge on its surface under physiological conditions, owing to the weak basicity of the NH_2 group, while the PC membrane is practically neutral.^{20,21} Unlike the PC membrane, the negative charge on the PG and PE membranes accounts for the observation that the relevant monolayer attracted the positively charged region of KcsA.

The distribution of KcsA was examined at pH 2.6 (Figure 3B, lower row), where KcsA is maximally activated (pH \sim 3).²² Under

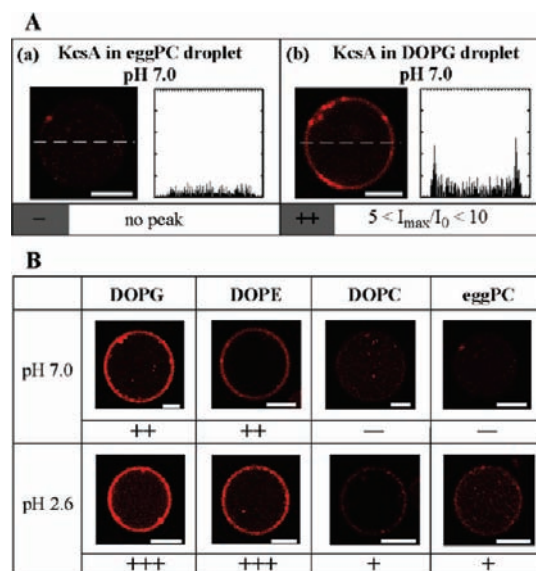


Figure 3. The distribution of the tagged-KcsA within the W/O droplet depends on the lipid type and pH. (A) Each box shows (left) fluorescent images of a droplet encapsulating KcsA and (right) their fluorescence–intensity profiles along the white dashed line. (B) We categorized these distributions of KcsA into four types according to the average value of the normalized maximum intensity I^* from 30 droplets: $-$ ($I^* \leq 1$); $+$ ($1 < I^* \leq 5$); $++$ ($5 < I^* \leq 10$); $+++$ ($I^* > 10$). Scale bar is 10 μm .

the acidic condition, the intensity of the peaks was further increased for the PG and PE droplets, and even for the PC droplets. In addition, no apparent difference in KcsA localization was observed between pH 3.8 and pH 2.6, and these are above and below the pK values of PG and PE in \sim 100 mM NaCl (2.9–3.5 and 2–3, respectively^{21,23,24}). This means that the interaction between the lipids and KcsA is not changed in the acidic condition, $2.6 < \text{pH} < 4$. From these results, it is indicated that KcsA channels have a direct interaction even with the lipid monolayer, and the interaction is enhanced under an acidic condition.

KcsA Insertion into Vesicles. The confocal images of the W/O droplets shown in Figure 3 demonstrate that KcsA is located at the interface but do not specify whether the channel remains at the interface between water and lipid head groups or penetrates into the hydrophobic region of the monolayer. To investigate the transfer and interaction of KcsA with the lipid bilayer, bilayer vesicles were formed as follows (Figure 1B). The W/O droplets lined with a lipid monolayer were transferred through the oil/water interface, where a lipid monolayer had formed beforehand. The monolayer interface encapsulates the monolayer-lined droplet when it passes through the interface, leading to bilayer formation. However, some of the vesicles remained below the interface. This procedure enabled the formation of asymmetric bilayers, although some combinations of lipid compositions for the outer and inner leaflets were not able to form vesicles. For example, a vesicle cannot be formed when PE is present in the outer leaflet because of the conical shape of PE.²⁵ In our procedure, the KcsA channels were either encapsulated in droplets (Figure 1B(a)) or included in the bulk water phase (Figure 1B(b)).

KcsA channels are inserted from outside the vesicles at pH 2.6. The confocal images of the vesicles with asymmetric lipid compositions in the outer/inner leaflets, i.e., eggPC/(DOPG,

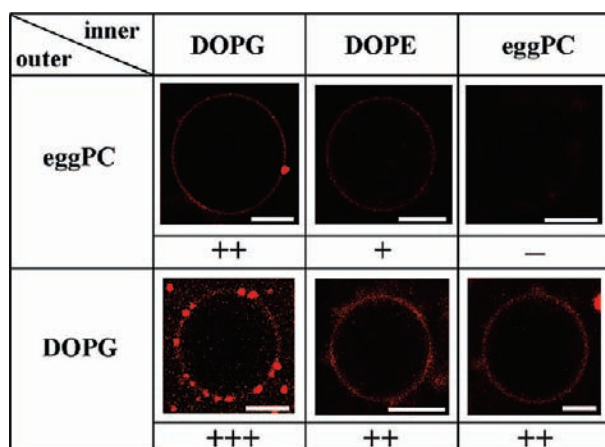


Figure 4. Confocal micrographs of asymmetric vesicles with KcsA inserted from the outside at pH 2.6. The indexes show the four KcsA distribution types, categorized from the average value of the normalized maximum intensity in 30 vesicles, I^* : - ($I^* \leq 1$); + ($1 < I^* \leq 3$); ++ ($3 < I^* \leq 6$); +++ ($I^* > 6$). Scale bar is 10 μm .

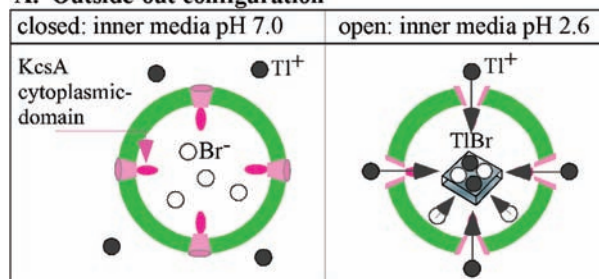
DOPE, and eggPC) and DOPG/(DOPG, DOPE, and eggPC), are shown in Figure 4. The localization of KcsA at the membrane was observed for vesicles containing PG or PE in either leaflet. The fluorescence intensity profiles of the vesicles were examined, and the normalized peak intensity, $I^* = I_{\text{max}}/I_0$, was calculated for 30 vesicles under each condition (Figure S6B). On the basis of the average values of I^* , the profiles were categorized into four types: -, $I^* \leq 1$; +, $1 < I^* \leq 3$; ++, $3 < I^* \leq 6$; and +++, $I^* > 6$.

We found that the density of KcsA for PG/PG vesicles was higher than that for PG/PC or PC/PG vesicles. It is likely that PC in the membrane hinders the accumulation of KcsA. How does KcsA interact with the lipid molecules at the membrane? In the following experiments, we examined the channel function of KcsA in the vesicle to elucidate whether KcsA is integrated into the bilayer or not.

Functional Activity and Orientation of Integrated KcsA in Vesicles. We developed a visual evaluation method to examine the channel activity of KcsA in the vesicle. In an earlier study, the presence and localization of potassium channels were examined by a thallium (Tl) crystallization method.¹⁸ This method relied on two features of Tl: (i) Tl^+ is permeable through potassium channels, including KcsA,¹⁹ and (ii) Tl^+ forms aggregates or crystal with Br^- . We used this method to examine the functionality of KcsA in vesicles. Moreover, this method allows a determination of KcsA orientation in vesicles for the following reasons. KcsA permeates Tl^+ when the pH-sensitive cytoplasmic domain (CPD) is bathed in acidic solution (Figure 5). The permeability of the oriented KcsA can be regulated by setting the intra- and extravesicular pH separately. Once opened, KcsA allows Tl^+ influx when KcsA is in either orientation on the vesicle membrane. This method is able to detect highly active channels embedded in the vesicular membrane.

First, KcsA channels were loaded from inside the vesicles (extravesicular Tl^+ ~ 10 mM; Figure 6A). When the intravesicular pH was 7.0, no crystal was observed in any of the vesicles, even when KcsA was localized at the membrane. When the intravesicular pH was 2.6 and the vesicle contained PG (eggPC/DOPG vesicles), TlBr crystals larger than 5 μm were observed. These crystals appeared bright under cross-polarized light

A. Outside-out configuration



B. Inside-out configuration

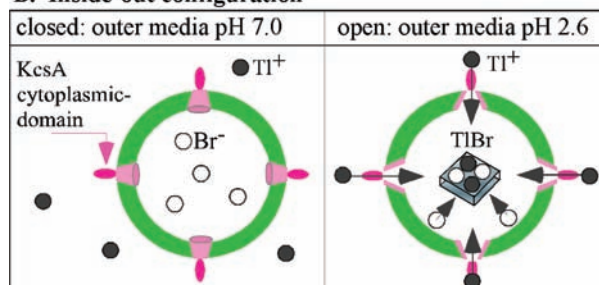


Figure 5. Schematic representation of the method used to examine the channel activity of KcsA reconstituted into vesicles (A) in an outside-out configuration and (B) an inside-out configuration. KcsA becomes permeable when its cytoplasmic domain is in acidic media. The open KcsA allows permeation of thallium ion Tl^+ into the vesicle, and intravesicular Tl^+ reacts with Br^- to generate TlBr.

(Figure S3, Supporting Information). Under microscopy, crystal growth was observed when the Tl^+ concentration was increased. At ~ 20 mM Tl, a large number of small crystal nuclei appeared within ~ 30 min after the formation of the vesicles and gradually grew in size (Figure S2C, Supporting Information). On the other hand, the addition of ~ 9 mM BaCl_2 (a potent KcsA blocker) inside the vesicles blocked the crystal growth (Figure S2D).

In these experiments the pH gradient was maintained for at least ~ 60 min after the formation of the vesicles (Figure S4C2, Supporting Information), even in the presence of KcsA in the open condition. We used PC/PC, PC/PE, and PC/PG (outer/inner leaflets) vesicles, because proton leakage through the membrane is enhanced in the presence of PG in the outer leaflet (Figure S4).

The above experimental results indicate that KcsA is oriented such that the pH-sensitive CPD is located inside the vesicle (outside-out configuration) (Figure 5A). On the other hand, no crystal was observed inside the PC/PE vesicles. This finding is consistent with the notion that the gating probability of KcsA is enhanced in the presence of PG.^{7,26}

Next, KcsA channels were loaded from outside of the vesicle (Figure 6B). When the extravesicular pH was 7.0, no crystals were observed. In contrast, crystals were observed when the pH of the bulk solution was 2.6 and the vesicle contained PG (eggPC/DOPG vesicles). Therefore, the outside insertion of KcsA led to the opposite orientation, i.e., the inside-out configuration (Figure 5B).

A closer inspection revealed clusters of KcsA channels on the membrane (up to 1 μm in size), below which the crystal hung. Interestingly, the size of the KcsA clusters is roughly proportional to that of the crystals. This clustering of KcsA channels has been previously reported in multilamellar giant vesicles composed of asolectin.²⁷

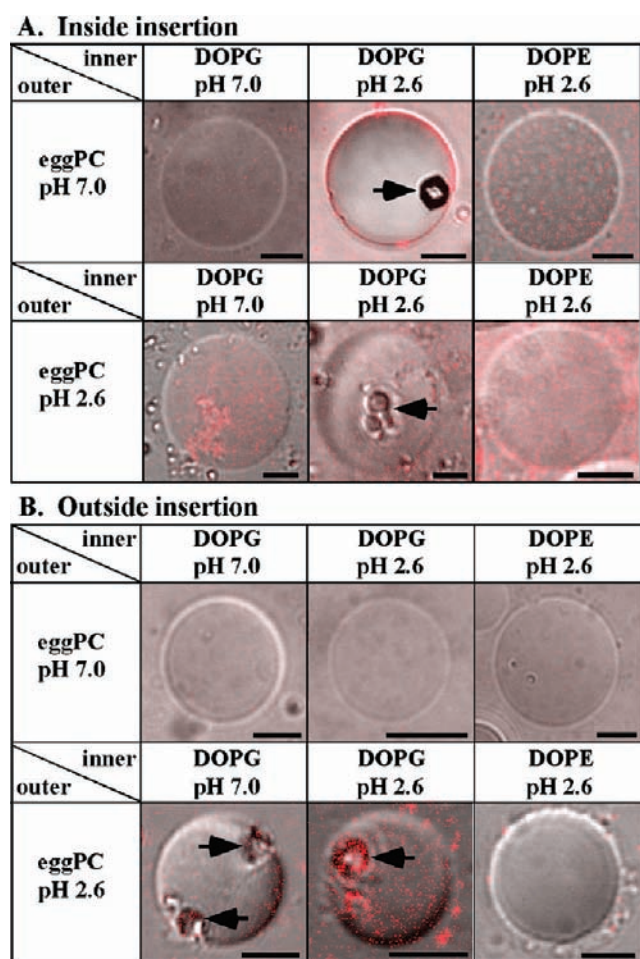


Figure 6. A crystallization test to examine the channel activity of KcsA loaded from (A) inside and (B) outside the vesicles. Confocal images combined with their phase-contrast images are shown, where red indicates the tagged-KcsA. The TLBr crystals, indicated by the arrows, are observed only in vesicles that contain DOPG and when the (A) inner or (B) outer media is acidic. Scale bar is 10 μm .

In the present study, the droplet-transfer method enabled an incorporation of KcsA in either orientation, i.e., the outside-out or inside-out configuration. In this procedure, solubilized KcsA is incorporated directly into GUVs. This is in contrast to the conventional method, which starts with tiny vesicles having a high curvature.^{2,3} There is a plausible explanation for the underlying mechanism of the directed insertion into GUVs. The CPD of KcsA is a bundle of α -helices extending toward the cytoplasmic side for 40 Å, which is almost the same size as the bilayer. This hydrophilic domain hardly transverses the hydrophobic membrane phase and is retained in the aqueous phase to which the solubilized KcsA was added.

To confirm this model, we used a CPD-truncated KcsA that retains the pH sensitivity⁶ and examined the TI crystallization. Similar to the full-length KcsA (Figure 6), crystals were observed in PG vesicles (Figure 7). In the CPD-truncated KcsA, we found that at acidic extravesicular pH, the KcsA inserted from the inside exhibited crystal formation even when the intravesicular pH was high (Figure 7A, right). Similarly, when the extravesicular pH was neutral, CPD-truncated KcsA inserted from the outside produced the crystal at intravesicular acidic pH (Figure 7B, left).

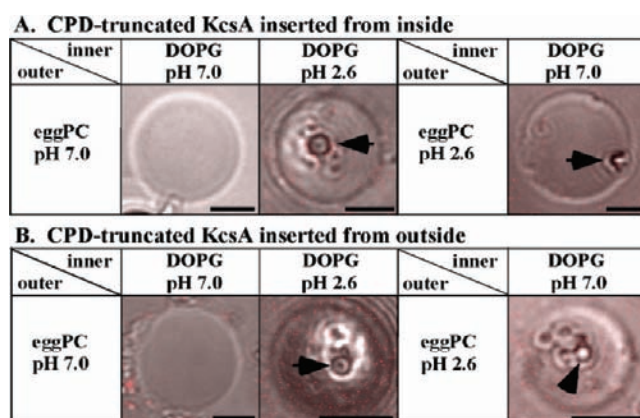


Figure 7. A crystallization test to examine the orientation of CPD-truncated KcsA inserted into the vesicles from (A) inside and (B) outside. The TLBr crystals, indicated by the arrows, are observed only in vesicles containing DOPG. In these vesicles, the channel was activated by acidic media from either the outside or inside. Scale bar is 10 μm .

Thus, we conclude that, in the absence of CPD, KcsA was randomly oriented in the liposome membrane. This is supporting evidence for the hypothesis that the CPD determines the orientation of KcsA.

In our present study, some of the vesicles remained anchored to the interface, and this issue can be circumvented by either the microfluidic-jetting method²⁸ or the use of a centrifuge.¹⁴ Our method is applicable to other transmembrane proteins having large hydrophilic portions on either the extracellular or intracellular side. Furthermore, by coupling this method with the phase-separation of lipids in vesicles containing the preferred lipids,²⁹ it should be possible to control the spatial distribution of membrane proteins in the desired orientation.^{30–33}

CONCLUSIONS

We have described a new method for the reconstitution of the potassium channel KcsA into GUVs in either an outside-out or inside-out configuration, by means of adding the solubilized KcsA in either intravesicular or extravesicular solution, using a droplet-transfer method. (1) W/O droplets lined with a lipid monolayer were prepared. When KcsA was encapsulated in the droplet, it accumulated at a monolayer of PG or PE but not a monolayer of PC. (2) GUVs were obtained by transferring droplets through the bulk oil/water interface with a preformed monolayer. The KcsA inserted from the inside or outside was spontaneously incorporated into the vesicles containing its preferred lipids, i.e., PG or PE. (3) The channel activity of the KcsA integrated into vesicles with PG at an acidic pH, which is necessary for gating, was detected using TI crystallization. Furthermore, the KcsA loaded from the inside or outside was in an outside-out or inside-out orientation, respectively. Finally, it was determined that the mechanism underlying the directed insertion was governed by the hydrophilic CPD. This method can be extended to other membrane proteins. On the basis of the above results, we propose here a new method for the orientated integration of membrane proteins. For membrane proteins having small extra- and intramembrane domains, adding a hydrophilic domain to one side results in directed insertion.

■ ASSOCIATED CONTENT

S Supporting Information. Additional figures of a single channel current of tagged-KcsA, time course of T1 crystallization in vesicles, time variation of pH gradient of vesicles, distribution of KcsA in droplets, and histogram of localization of KcsA in droplets or vesicles. This information is available free of charge via the Internet at <http://pubs.acs.org>.

■ AUTHOR INFORMATION

Corresponding Author

yanagisawa@phys.kyushu-u.ac.jp; yoshikaw@scphys.kyoto-u.ac.jp;
oiki-fki@umin.ac.jp

Present Addresses

^{||}Department of Physics, Graduate School of Science, Kyushu University, Fukuoka 812-8581, Japan.

■ ACKNOWLEDGMENT

This work was supported in part by the Japan Society for the Promotion of Science (JSPS) under a Grant-in-Aid for Creative Scientific Research (Project No. 18GS0421). M.Y. is grateful for support from a JPSP Fellowship (Grant-in-Aid for Young Scientists; No. 22-940). We also thank Kei Fujiwara, Yuko T. Sato, and Kingo Takiguchi for their fruitful discussions.

■ REFERENCES

- (1) Lee, A. G. *Biochim. Biophys. Acta* **2004**, *1666*, 62–87.
- (2) Racker, E. *Methods Enzymol.* **1979**, *55*, 699–711.
- (3) Eytan, G. D. *Biochim. Biophys. Acta* **1982**, *694*, 185–202.
- (4) Fung, B. K.; Hubbell, W. L. *Biochemistry* **1978**, *17*, 4396–4402.
- (5) Cuello, L. G.; Romero, J. G.; Cortes, D. M.; Perozo, E. *Biochemistry* **1998**, *37*, 3229–3236.
- (6) Doyle, D. A.; Morais Cabral, J.; Pfuetzner, R. A.; Kuo, A.; Gulbis, J. M.; Cohen, S. L.; Chait, B. T.; MacKinnon, R. *Science* **1998**, *280*, 69–77.
- (7) Heginbotham, L.; LeMasurier, M.; Kolmakova-Partensky, L.; Miller, C. J. *Gen. Physiol.* **1999**, *114*, 551–560.
- (8) Heginbotham, L.; Kolmakova-Partensky, L.; Miller, C. J. *Gen. Physiol.* **1998**, *111*, 741–749.
- (9) Valiyaveetil, F. I.; Zhou, Y.; MacKinnon, R. *Biochemistry* **2002**, *41*, 10771–10777.
- (10) Reusch, R. N. *Biochemistry* **1999**, *38*, 15666–15672.
- (11) Iwamoto, M.; Shimizu, H.; Inoue, F.; Konno, T.; Sasaki, Y. C.; Oiki, S. *J. Biol. Chem.* **2006**, *281*, 28379–28386.
- (12) Shimizu, H.; Iwamoto, M.; Konno, T.; Nihei, A.; Sasaki, Y. C.; Oiki, S. *Cell* **2008**, *132*, 67–78.
- (13) Pautot, S.; Frisken, B. J.; Cheng, J. X.; Xie, X. S.; Weitz, D. A. *Langmuir* **2003**, *19*, 10281–10287.
- (14) Pautot, S.; Frisken, B. J.; Weitz, D. A. *Proc. Natl. Acad. Sci. U.S.A.* **2003**, *100*, 10718–10721.
- (15) Yamada, A.; Yamanaka, T.; Hamada, T.; Hase, M.; Yoshikawa, K.; Baigl, D. *Langmuir* **2006**, *22*, 9824–9828.
- (16) Hamada, T.; Miura, Y.; Komatsu, Y.; Kishimoto, Y.; Vestergaard, M.; Takagi, M. *J. Phys. Chem. B* **2008**, *112*, 14678–14681.
- (17) Kato, A.; Shindo, E.; Sakae, T.; Tsuji, A.; Yoshikawa, K. *Biophys. J.* **2009**, *97*, 1678–1686.
- (18) Lopatin, A. N.; Makhina, E. N.; Nichols, C. G. *Biophys. J.* **1998**, *74*, 2159–2170.
- (19) LeMasurier, M.; Heginbotham, L.; Miller, C. J. *Gen. Physiol.* **2001**, *118*, 303–314.
- (20) Egawa, H.; Furusawa, K. *Langmuir* **1999**, *15*, 1660–1666.
- (21) Boggs, J. M. *Can. J. Biochem.* **1980**, *58*, 755–770.
- (22) Chakrapani, S.; Cordero-Morales, J. F.; Perozo, E. *J. Gen. Physiol.* **2007**, *130*, 465–478.
- (23) Watts, A.; Harlos, K.; Maschke, W.; Marsh, D. *Biochim. Biophys. Acta* **1978**, *510*, 63–74.
- (24) van Dijk, P. W.; de Kruijff, B.; Verkleij, A. J.; van Deenen, L. L.; de Gier, J. *Biochim. Biophys. Acta* **1978**, *512*, 84–96.
- (25) Israelachvili, J. N.; Marcelja, S.; Horn, R. G. *Q. Rev. Biophys.* **1980**, *13*, 121–200.
- (26) Marius, P.; Zagnoni, M.; Sandison, M. E.; East, J. M.; Morgan, H.; Lee, A. G. *Biophys. J.* **2008**, *94*, 1689–1698.
- (27) Molina, M. L.; Barrera, F. N.; Fernandez, A. M.; Poveda, J. A.; Renart, M. L.; Encinar, J. A.; Riquelme, G.; Gonzalez-Ros, J. M. *J. Biol. Chem.* **2006**, *281*, 18837–18848.
- (28) Stachowiak, J. C.; Richmond, D. L.; Li, T. H.; Liu, A. P.; Parekh, S. H.; Fletcher, D. A. *Proc. Natl. Acad. Sci. U.S.A.* **2008**, *105*, 4697–4702.
- (29) Yanagisawa, M.; Imai, M.; Taniguchi, T. *Phys. Rev. Lett.* **2008**, *100*, 148102.
- (30) Seeger, H. M.; Bortolotti, C. A.; Alessandrini, A.; Facci, P. *J. Phys. Chem. B* **2009**, *113*, 16654–16659.
- (31) Litt, J.; Padala, C.; Asuri, P.; Vutukuru, S.; Athmakuri, K.; Kumar, S.; Dordick, J.; Kane, R. S. *J. Am. Chem. Soc.* **2009**, *131*, 7107–7111.
- (32) Yu, Y.; Vroman, J. A.; Bae, S. C.; Granick, S. *J. Am. Chem. Soc.* **2010**, *132*, 195–201.
- (33) Hamada, T.; Morita, M.; Kishimoto, Y.; Komatsu, Y.; Vestergaard, M.; Takagi, M. *J. Phys. Chem. Lett.* **2010**, *1*, 170–173.